

Density classification performance of the Gacs-Kurdyumov-Levin four-state cellular automaton model IV

J. Ricardo G. Mendonça^{a,*} and Rolf E. O. Simões^{b,†}

^a*Escola de Artes, Ciências e Humanidades, Universidade de São Paulo
Rua Arlindo Bettio 1000, Ermelino Matarazzo, 03828-000 São Paulo, SP, Brazil*

^b*Lab. Assoc. de Computação e Matemática Aplicada, Instituto Nacional de Pesquisas Espaciais
Avenida dos Astronautas 1758, Jd. da Granja, 12227-010 São José dos Campos, SP, Brazil*

Abstract

Almost four decades ago, Gacs, Kurdyumov, and Levin introduced three different cellular automata to investigate whether one-dimensional nonequilibrium interacting particle systems are capable of displaying phase transitions and, as a by-product, introduced the density classification problem in the cellular automata literature. Their model II became a well known model in theoretical computer science and statistical mechanics. The other models, however, did not receive much attention. Here we characterize the density classification performance of Gacs, Kurdyumov, and Levin's model IV, a four-state cellular automaton with three absorbing states, by Monte Carlo simulations. We show that model IV compares well with its sibling model II in the density classification task: the additional states slow down the convergence to the majority state but confer a slight advantage in classification performance. We also investigated the performance of model IV under the influence of noise and found signs of an ergodic-nonergodic phase transition at some small finite positive level of noise, although the evidences are not entirely conclusive. We obtain an upper bound on the critical point for such a transition, if any.

Keywords: Density classification problem · positive probabilities conjecture · ergodic cellular automata · noise · spatially distributed computing

PACS: 05.70.Fh · 64.60.De · 64.60.Ht

*Email: jricardo@usp.br

†Email: rolf.simoes@inpe.br

1 Introduction

In 1978, Gacs, Kurdyumov, and Levin (GKL) introduced three different cellular automata (CA), which they called models II, IV, and VI, to investigate whether nonequilibrium interacting particle systems are capable of displaying phase transitions [1, 2]. Their objective was to examine the so-called “positive probabilities conjecture,” according to which one-dimensional systems with short-range interactions and positive transition probabilities are always ergodic [3, 4, 5, 7, 6, 10, 8, 9, 11]. This conjecture has been disproved—much to the awe of the practising community—many times since then, with the introduction of several models that have become archetypal models in theoretical computer science and nonequilibrium statistical mechanics [12, 13, 14, 15, 16, 17, 18, 19, 20, 21, 22, 23, 24, 25, 26, 27, 28].

As a by-product of their investigations, GKL introduced the density classification problem in the cellular automata literature. The density classification problem consists in classifying arrays of symbols according to their initial density using local rules, and is completed successfully if a correct verdict as to which was the initial majority state is obtained in time at most linear in the size of the input array. Density classification is a nontrivial task for CA in which cells interact over finite neighbourhoods, because then the cells have to achieve a global consensus cooperating locally only. Ultimately, that means that information should flow through the entire system, be processed by the cells, and be not destroyed or become incoherent in the process—entropy must loose to work, a relevant property in the theoretical analysis of data processing and storage under noise [14, 15, 16]. For one-dimensional locally interacting systems of autonomous and memoryless cells, emergence of collective behavior is required in these cases. In this context, GKL model II has been extensively scrutinized as a model system related with the concepts of emergence, communication, efficiency, and connectivity [29, 30, 31, 32, 33, 34, 35, 36, 37, 38, 39]. Current trends, advances and open problems related with the density classification problem are reviewed in [40, 41, 42, 43, 44, 45].

In this paper we characterize the density classification performance of Gacs, Kurdyumov, and Levin’s model IV, a four-state cellular automaton with three absorbing states, by Monte Carlo simulations. To our knowledge, the model never received a thorough examination of its basic dynamics and properties since its proposition. We show that GKL model IV compares well with its sibling model II in the density classification task, although it takes longer to converge to the right answer. We also investigate the performance of model IV under the influence of noise and show that, most likely, it displays an ergodic-nonergodic transition at some finite small level of noise, although the evidences are not conclusive.

The paper goes as follows: in Section 2 we introduce the GKL model IV, describe its transition rules, and discuss some of its known properties. In Section 3 we describe our Monte Carlo simulations and discuss the density classification performance of the model in its deter-

ministic version, including a comparison with GKL model II, while in Section 4 we examine the behavior of the model under the influence of noise. In Section 5 we summarize our findings and discuss our results. The complete rule table of GKL model IV is given in an appendix.

2 The Gacs, Kurdyumov, and Levin's CA model IV

Gacs, Kurdyumov, and Levin's model IV (GKL-IV for short) is a four-state CA with state space given by $\Omega_\Lambda = \{\rightarrow, \leftarrow, \uparrow, \downarrow\}^\Lambda$, with $\Lambda \subseteq \mathbb{Z}$ a finite array of $|\Lambda| = L \geq 1$ cells under periodic boundary conditions, and transition function $\Phi_{\text{IV}} : \Omega_\Lambda \rightarrow \Omega_\Lambda$ that given the state $\mathbf{x}^t = (x_1^t, x_2^t, \dots, x_L^t)$ of the CA at instant t determines the state $\mathbf{x}^{t+1} = [\Phi_{\text{IV}}(\mathbf{x}^t)]_i = \phi_{\text{IV}}(x_{i-1}^t, x_i^t, x_{i+1}^t)$ of the CA at instant $t + 1$ by the rules

$$\phi_{\text{IV}}(\rightarrow, x_i, x_{i+1}) = \rightarrow, \quad \text{if } x_i, x_{i+1} \neq \leftarrow, \quad (1a)$$

$$\phi_{\text{IV}}(x_{i-1}, \rightarrow, x_{i+1}) = \begin{cases} \downarrow, & \text{if } x_{i-1} \in \{\leftarrow, \uparrow\}, \\ \rightarrow, & \text{otherwise,} \end{cases} \quad (1b)$$

$$\phi_{\text{IV}}(x_{i-1}, x_i, x_{i+1}) = \uparrow, \quad \text{if } x_i \in \{\uparrow, \downarrow\} \text{ and rule (1a) does not apply,} \quad (1c)$$

where we have omitted the time index t from the x_i^t since the rules do not depend on time.

Rules (1a)–(1c) are redundant—for example, transitions $\phi_{\text{IV}}(\rightarrow, \rightarrow, \{\rightarrow, \uparrow, \downarrow\})$ are defined both by rules (1a) and (1b)—and insufficient, since they define only 42 of the 64 possible transitions. The missing transitions must be determined by the additional reflection rule

$$\phi_{\text{IV}}(x_{i-1}, x_i, x_{i+1}) = \phi_{\text{IV}}(x_{i+1}^*, x_i^*, x_{i-1}^*)^*, \quad (2)$$

with $\rightarrow^* = \leftarrow$, $\leftarrow^* = \rightarrow$, $\uparrow^* = \uparrow$, and $\downarrow^* = \downarrow$. The reflection rule supplements rules (1a)–(1c) in their order of appearance and does not substitute a transition that has already been defined. We can represent these prescriptions schematically by the precedence chain $(1a) \preceq (1a)^* \preceq (1b) \preceq (1b)^* \preceq (1c) \preceq (1c)^*$. Since the GKL-IV rules are somewhat unwieldy, we give the complete rule table of the CA in A.

In [2], the authors state that the states \rightarrow and \leftarrow are attracting states for models II and IV, further noticing that “evidently [models II and IV] do not have other attracting states.” It happens, however, that GKL-IV has three absorbing states, as it can be seen from the transitions $\phi(\rightarrow, \rightarrow, \rightarrow) = \rightarrow$, $\phi(\leftarrow, \leftarrow, \leftarrow) = \leftarrow$, and $\phi(\uparrow, \uparrow, \uparrow) = \uparrow$. That the states $(\rightarrow, \rightarrow, \dots, \rightarrow)$ and $(\leftarrow, \leftarrow, \dots, \leftarrow)$ are attracting is a theorem of GKL [2]. The state $(\uparrow, \uparrow, \dots, \uparrow)$, despite being absorbing, may not be attracting, since it may not be true that if we disturb it in finitely many places it will recur in finite time. In our simulations on relatively small systems, however, we observed the convergence of the GKL-IV CA to the state $(\uparrow, \uparrow, \dots, \uparrow)$ many times. Rough initial estimates indicated that for random, uncorrelated initial configurations in which each

cell initially gets one of the four possible states with equal probabilities, the final configuration converges to $(\uparrow, \uparrow, \dots, \uparrow)$ about 1% of the times. We thus asked whether GKL-IV can classify initial configurations with majority of cells in state \uparrow , even if it was not designed for the task. As we will see in Section 3 the answer is nearly never, corroborating the affirmations in [2].

3 Density classification performance of GKL-IV

Let N_s be the number of cells in the state $s \in \{\rightarrow, \leftarrow, \uparrow, \downarrow\}$, with $N_{\rightarrow} + N_{\leftarrow} + N_{\uparrow} + N_{\downarrow} = L$, the size of the array. Given an initial assignment of the numbers N_s , the main observables of the CA are the empirical time-dependent number of cells in state s given by

$$N_s(t) = \sum_{i=1}^L \delta(x_i^t, s), \quad (3)$$

where $\delta(\cdot, \cdot)$ is the Kronecker delta symbol. GKL argued in [2] that in the stationary state either the state \rightarrow or the state \leftarrow completely dominates the CA, with the dominance depending on which state, \rightarrow or \leftarrow , respectively, prevails in the initial configuration; states \uparrow and \downarrow are washed out by the dynamics and do not survive to the stationary state.

We assess the density classification performance of the GKL-IV CA by Monte Carlo simulations as follows. We set the array size L to a multiple of 4 and then assign $L/4$ randomly chosen cells to each of the states \uparrow and \downarrow , $L/4 + k$ cells to state \rightarrow , and $L/4 - k$ cells to state \leftarrow , with k an integer parameter that can be varied in the range $-L/4 \leq k \leq L/4$. Given the density classification property of GKL-IV, we expect that when $k > 0$ the stationary state will be the all \rightarrow state while when $k < 0$ the stationary state will be the all \leftarrow state. We then evolve the CA array and track the empirical densities until at some time t^* either $N_{\rightarrow}(t^*) = L$ or $N_{\leftarrow}(t^*) = L$. If initially $k > 0$ ($k < 0$) and the stationary state becomes the all \rightarrow (respectively, all \leftarrow) state, then GKL-IV has classified the initial state successfully, otherwise it has failed. We also consider that the CA failed if after $4L$ time steps the array did not converge to one of those two states, but this did not happen in our simulations. When $k = 0$, we compute the performance of the GKL-IV array as the number of times that it converges to the all \rightarrow state. The choice between the all \rightarrow or the all \leftarrow states in this case is irrelevant because the GKL-IV rules are reflection-symmetric with respect to these states and our array is periodic; see Table I. For each value of k the experiment is repeated 10,000 times and the statistics collected; the results appear in Figure 1. For comparison, results for the sibling GKL model II (GKL-II for short) are also displayed in Figure 1. GKL-II is a two-state CA that evolves by the following rule [2, 20]: if the state of the cell at instant t is $+1$ (or, equivalently, \rightarrow), then at instant $t + 1$ it takes the majority vote of itself and the first and the third neighbors to its right, otherwise, if the state of the cell at instant t is -1 (or \leftarrow), it takes at instant $t + 1$ the majority state of the same neighborhood

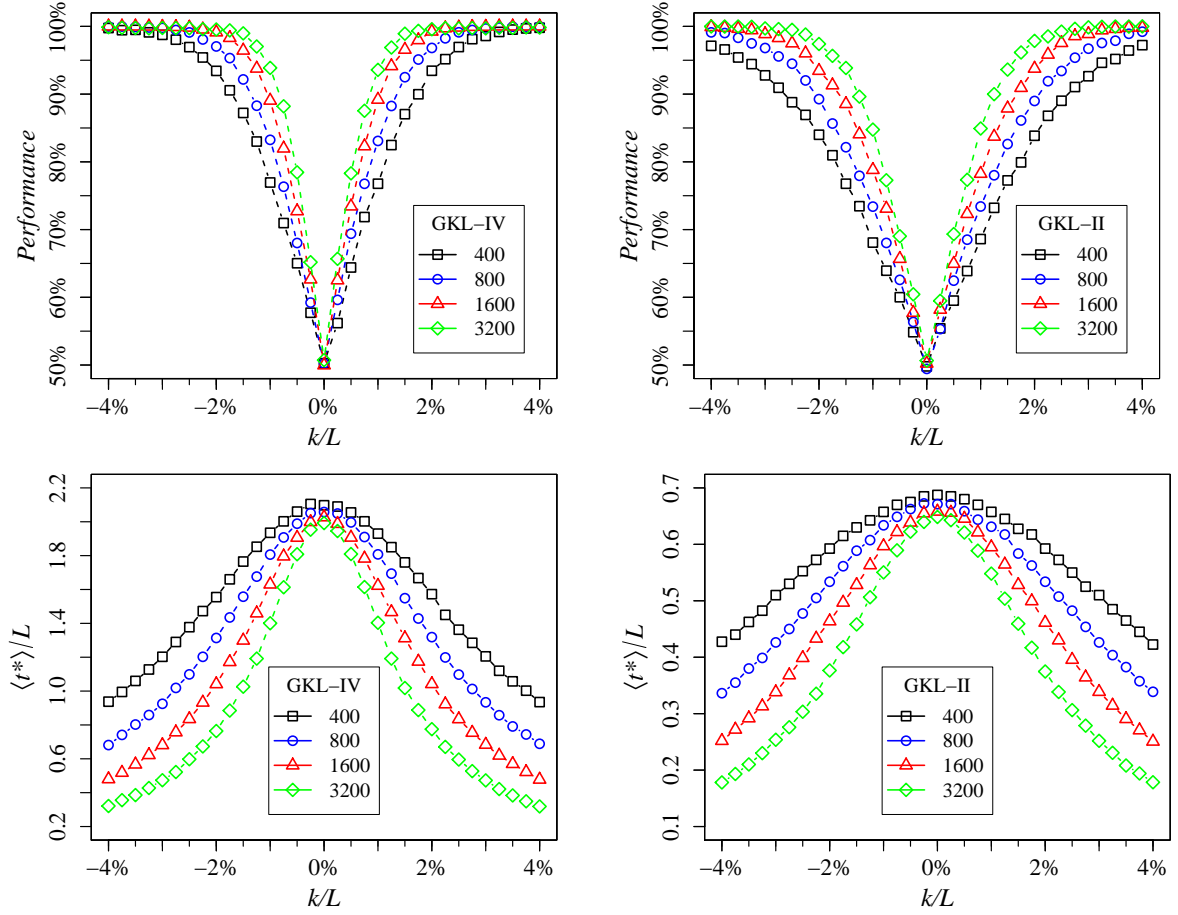


Figure 1: Density classification performance of GKL-IV and GKL-II, shown for comparison. Parameter $k = \frac{1}{2}(N_{\rightarrow} - N_{\leftarrow})$ represents the imbalance between the number of cells in states \rightarrow and \leftarrow in the initial configuration. Upper panels: neither GKL-II nor GKL-IV is a perfect classifier, but GKL-IV performs better. Lower panels: average time $\langle t^* \rangle$ to converge to the stationary state in units of the length of the CA. In this case, GKL-IV performs worse than the simpler GKL-II. In all cases data correspond to averages over 10,000 samples; error bars are smaller than the symbols shown.

but in the opposite direction. In symbols,

$$x_i^{t+1} = [\Phi_{\Pi}(\mathbf{x}^t)]_i = \phi_{\Pi}(x_i^t, x_{i+s}^t, x_{i+3s}^t) = \text{maj}(x_i^t, x_{i+s}^t, x_{i+3s}^t), \quad s = x_i^t = \pm 1. \quad (4)$$

The GKL-II rule is not nearest-neighbor but observes a generalization of the reflection rule (2), to wit, $\phi_{\Pi}(x_i, x_j, x_k) = \phi_{\Pi}(x_{\sigma(i)}^*, x_{\sigma(j)}^*, x_{\sigma(k)}^*)^*$, where $x^* = -x$ and σ is any permutation of i, j, k .

We see from Figure 1 that GKL-IV is not a perfect classifier: for random initial configurations, sometimes it converges to the wrong answer. Otherwise, when the imbalance k/L between the \rightarrow and the \leftarrow states in the initial state is larger than $\sim 2\%$, the GKL-IV classification performance exceeds 95%, an excellent result. This performance is considerably better than the one for GKL-II, that at $k/l = 2\%$ is only about $\sim 85\%$ and reaches the 95% mark only for

$k/L \gtrsim 3\%$.

The lower panels in Figure 1 display the time needed to converge to the stationary state as a function of k/L . We see that as the imbalance becomes smaller the time to converge grows, but it never grows more than linearly with the size of the array. Even for large instances of the problem (large L) in the difficult region $k/L \ll 1$, GKL-IV converges fast to the solution. In this regard, however, GKL-II exceeds GKL-IV almost by a factor of 3. It seems that the additional states of GKL-IV provide more “error-correction,” while at the same time retarding the convergence to the majority state; this point is further discussed in Sections 4.1 and 5.

We found that GKL-IV sometimes converges to the all \uparrow state, which is also one of its absorbing configurations. For relatively small array sizes, $L \sim 40\text{--}80$, and random initial configurations in which each cell starts in one of the four possible states with equal probability $1/4$, we observed that the array converges to the state $(\uparrow, \uparrow, \dots, \uparrow)$ approximately 1% of the times. To quantify this behavior, we performed the following experiment: we initially assign a fraction $\frac{1}{4} \leq f \leq 1$ of the L cells to state \uparrow and distribute the remaining $(1-f)L$ cells randomly to the other three possible states (such that $N_{\uparrow}(0) = fL$ exactly and, on average, $N_s(0) = \frac{1}{3}(1-f)L$ for each of the other possible states), evolve the dynamics and observe the approach to stationarity. The results are summarized in Figure 2. As we can see from that figure, even with as much as 85% of the cells initially in the state \uparrow GKL-IV cannot really classify initial states with majority of cells in the state \uparrow except for the smallest arrays—and even in these cases, only very badly, at an unacceptable rate of $\sim 10\%$. On the other hand, and by the same token, GKL-IV becomes confused and cannot classify the majority of states \rightarrow or \leftarrow in the presence of an overwhelming number of \uparrow states. Figure 2 thus complements the information contained in Figure 1 in that the classification power of GKL-IV does not depend solely on the imbalance between the number of cells in the states \rightarrow and \leftarrow , as it necessarily is the case with its sibling GKL-II model, it also depends, although very weakly, on the number of cells in the \uparrow state. We did not find anything similar for the state \downarrow , that is neither attractive nor absorbing.

4 The GKL-IV model under noise

A CA with rules depending on a random variable becomes a probabilistic, or stochastic, CA (PCA). Let us denote the probabilistic transition function of the GKL-IV model under noise by $\Phi_{\text{IV}}^{(\alpha)}$, where the real parameter $\alpha \in [0, 1]$ denotes the level of noise imposed to the dynamics. If $\alpha = 0$, GKL-IV becomes the deterministic CA given by transition rules (1)–(2), otherwise with probability $\alpha > 0$ the transition rules fail in some specific manner, leading to an evolved state that may be at variance with the one prescribed by the deterministic transition rules. In their paper [2], GKL considered mainly random writing errors: at every time step, with probability $1 - \alpha$ the transition follows rules (1)–(2) and with probability α the final state is chosen at

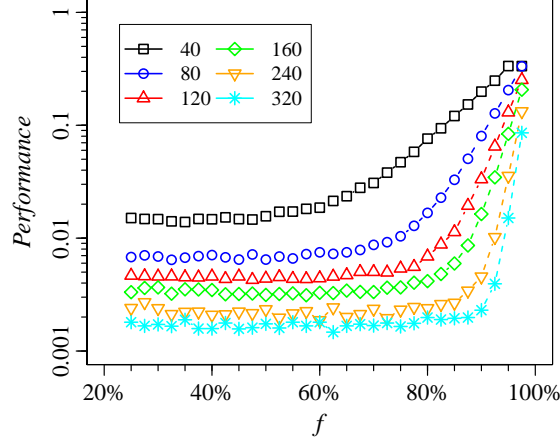


Figure 2: Density classification performance of GKL-IV with respect to the \uparrow state. Each point corresponds to an average over 100,000 samples; error bars are of the order of the size of the symbols and are not displayed because they are not indispensable to the argument. Note that unless the density of cells initially in the state \uparrow is very large, say, $\gtrsim 90\%$, the final, stationary state seldom converges to the absorbing state $(\uparrow, \uparrow, \dots, \uparrow)$ but for the smallest arrays.

random with equal probabilities. In other words, for GKL-IV model under noise level α , at every time step the probability of writing the new state to a cell according to the rules is $(1 - \alpha) + \frac{1}{4}\alpha$, while the probability of doing it incorrectly is $\frac{3}{4}\alpha$.

A PCA is ergodic if it eventually forgets its initial state, meaning that it has a unique invariant measure—a unique probability distribution of states over the configuration space of the model that does not change under the dynamics. Remarkably, GKL found by means of numerical experiments evidence that GKL-IV may be nonergodic below a certain small level of noise $\alpha_c \approx 0.05$ [2]. If true, this would provide a counterexample to the positive probabilities conjecture, according to which all one-dimensional PCA and related continuous-time interacting particle systems with positive rates, short-range interactions and finite local state space are ergodic. This conjecture is deeply rooted in the theory of Markov processes and has a counterpart in the well-known statistical physics lore that one-dimensional systems do not display phase transitions at finite ($T > 0$) temperature [13, 14, 15, 16, 17]. It took nearly three decades to disprove this conjecture in general [21, 22, 23], while counterexamples also appeared in the physics literature [17, 24, 25, 26, 27, 28]. The roles played by the size of the rule spaces, symmetries, number of absorbing states, irreversibility and the thermodynamic limit in the phenomenon are still under debate.

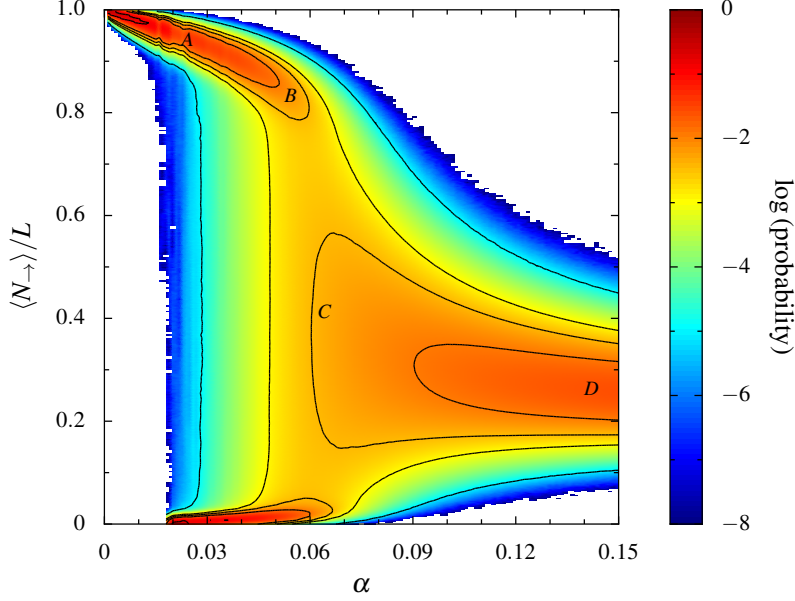


Figure 3: Heatmap and some level curves of the probability density of the majority state in the stationary state of the GKL-IV PCA under noise for an array of size $L = 400$. For each of the 150 levels of noise in the interval $0 < \alpha \leq 0.15$ ($\Delta\alpha = 0.001$), the probability density histogram was obtained from 100 million samples. In the figure, the letters mark the points A (0.012, 0.95), B (0.05, 0.84), C (0.065, 0.40), and D (0.14, 0.25).

4.1 Empirical stationary density

Little is known about the ergodicity of GKL-IV beyond the loose lower bound $\alpha_c \approx 0.05$ mentioned in [2], in contrast with the same problem for GKL-II [21, 22, 23, 20, 39]. To improve this situation, we performed relatively large simulations of GKL-IV under noise to verify whether there may be some sort of ergodic-nonergodic transition upon the variation of α .

Our simulations ran as follows. For a given level of noise α , we initialize a PCA of length $L = 400$ with all cells in the state \rightarrow , relax the initial state (run the dynamics) for $4L$ time steps, with one time step equal to the simultaneous update of all cells of the PCA, and start sampling the number N_{\rightarrow} of cells in the state \rightarrow in the PCA every 5 time steps. We collected 10^8 samples of the stationary state for each level of noise in the range $0 < \alpha \leq 0.15$ in steps of $\Delta\alpha = 0.001$ and the results are displayed as a density plot in Figure 3.

Figure 3 clearly displays the two extreme behaviors expected of the noisy GKL-IV. When $\alpha = 0$, the distribution of $\langle N_{\rightarrow} \rangle / L$ is a zero-width distribution concentrated at 1. At the other extreme, when the level of the noise is high, in our case $\alpha \gtrsim 0.12$, all the states become equiprobable and the density $\langle N_{\rightarrow} \rangle / L$ concentrates around $1/4$ with a more or less symmetric distribution that becomes sharper as α increases. The difficult question is whether there is a finite positive $\alpha_c > 0$ such that the noisy GKL-IV is ergodic above α_c and nonergodic below it. Figure 3 indicates that the probability distribution of $\langle N_{\rightarrow} \rangle / L$ becomes bimodal at $\alpha \approx 0.05$, with one peak

concentrated near the majority of states \rightarrow and the other peak near the majority of states \leftarrow , becoming narrower as $\alpha \searrow 0$. We also see that flipping between the two majority phases ceases completely, at least within the span of 5×10^8 time steps of our simulations, about $\alpha \approx 0.018$. These seem to indicate that the noisy GKL-IV may be nonergodic for some finite α .

Figure 4 depicts typical space-time diagrams of the noisy GKL-IV for some selected levels of noise. In diagram A ($\alpha = 0.012$, upper left corner), the state of the PCA just fluctuates about the majority state of \rightarrow to which it would have converged if it were not for the noise. Small islands of contiguous \uparrow (white) states that form could in principle foster the spread of the minority state \leftarrow (purple), but these islands are too small and short lived to make any difference. Ergodicity at this level of noise would imply that an island of the minority phase (or of the \uparrow (white) state) large enough to thrive in the background of the majority phase and noise can form randomly—an exceedingly unlikely event. The overall result is a spotted spatiotemporal pattern of the majority state that on average occupy $\sim 95\%$ of the cells.

As the noise α increases, larger islands of \uparrow (white) states form and the states \rightarrow (yellow) and \leftarrow (purple) tend to coexist for longer periods. In diagram B ($\alpha = 0.05$, upper right corner of Figure 4), we see larger islands of \uparrow (white) states allowing \leftarrow (purple) states to spread to the left until being annihilated. Eventually, however, those sliders meet to form bigger ones, survive for longer periods and become the majority state. Such an event was captured in diagram C ($\alpha = 0.065$, lower left corner of Figure 4). Note how the initially majority of states \rightarrow (yellow) in the top of the diagram is superseded by the \leftarrow (purple) states after some time; at the bottom of diagram C the \leftarrow (purple) states occupy $\sim 60\%$ of the cells. The PCA has flipped between two majority phases, an indication that at $\alpha = 0.065$ it is ergodic.

Finally, under the presence of strong noise, the PCA loses almost all structure except very locally and for short times. This can be seen in diagram D ($\alpha = 0.14$, lower right corner of Figure 4). Although islands of the attractive states \rightarrow (yellow) and \leftarrow (purple) endure more than islands of the other two states (and this is particularly true of the \downarrow (black) states), on average all four states are present approximately in the same amount. Note, in Figure 3, how the stationary probability density at C still displays a bimodal profile, while at D it is clearly a single-peaked distribution centered at $\sim 1/4$.

4.2 Flipping times

It is possible to qualitatively spot an ergodic phase by the analysis of the flipping times between the different stationary configurations of the model. The idea is that this quantity diverges as “potential barriers” grow between the metastable configurations of the system as it gets larger, with the system getting trapped deeper and deeper inside one configuration until ultimately ergodicity is broken in the limit of an infinite system. Based on an analogy between the flipping

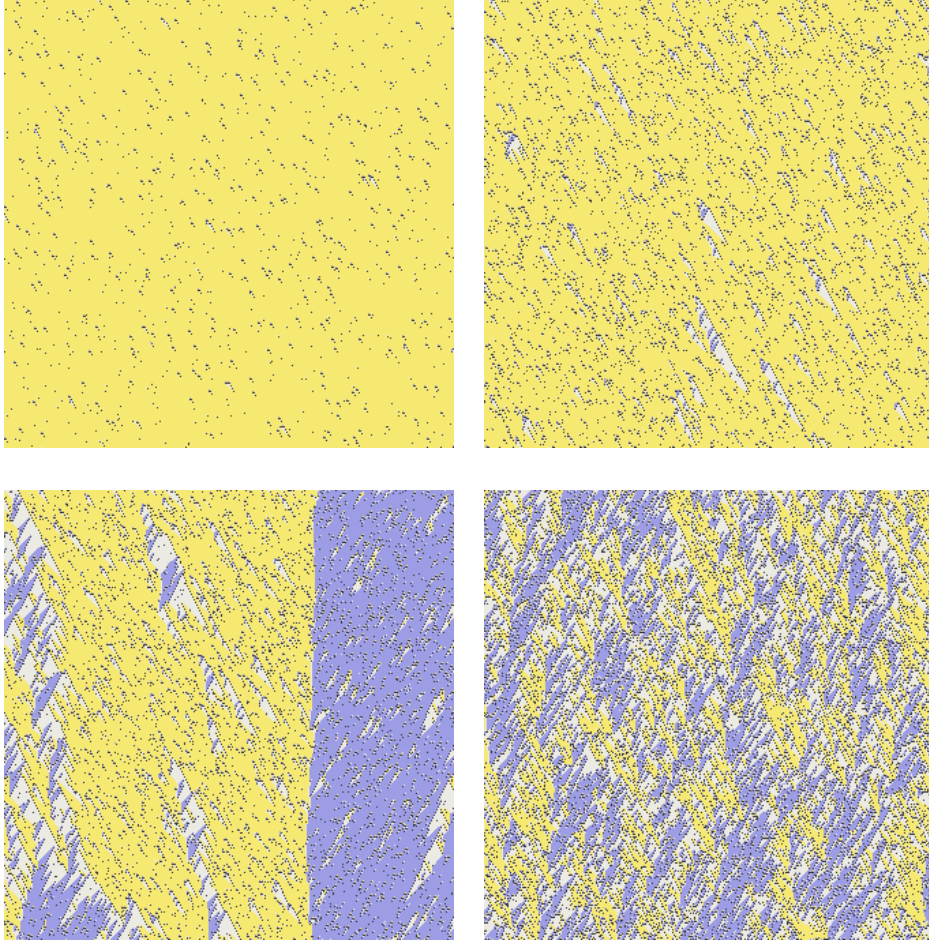


Figure 4: Sample runs of GKL-IV under noise level α in the stationary state. In left-to-right, top-to-bottom order, the space-time diagrams (time flows downward) correspond to sample runs of typical configurations found around the loci A , B , C and D indicated in Figure 3. The color coding reads yellow $\equiv \rightarrow$, purple $\equiv \leftarrow$, white $\equiv \uparrow$, and black $\equiv \downarrow$. Note how white regions of \uparrow states tend to cluster, while black regions (mostly just isolated spots) of \downarrow states straggle throughout.

time $\tau(L, \alpha)$ between the majority phases of a PCA of L cells subject to noise level α and the correlation length $\xi_{\parallel}(L, T)$ of a 2D equilibrium interacting classical spin model of linear size L at temperature T (see [20, 39, 27, 28, 46] for details), we expect that

$$\tau(L, \alpha) \sim \exp(u(L, \alpha)), \quad (5)$$

possibly with an algebraic prefactor. A nonergodic dynamics implies that $\tau(L, \alpha)$ diverges as $L \nearrow \infty$, while for an ergodic dynamics $u(L, \alpha)$ remains bounded in L , signaling that the PCA forgets about its initial condition in finite time, wandering over the entire configuration space and making the invariant measure unique. Clearly, for GKL-IV $\tau(L, \alpha)$ must diverge at $\alpha = 0$.

We measured $\tau(L, \alpha)$ for the noisy GKL-IV as follows. For a given level of noise α , we initialize the PCA with all cells in the state \rightarrow and run the dynamics until a state with majority of

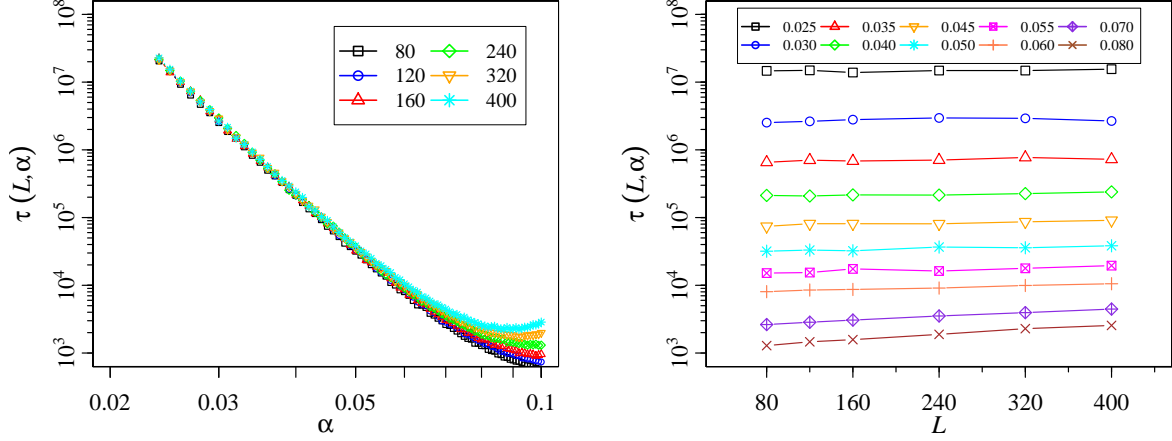


Figure 5: Left panel: the flipping times $\tau(L, \alpha)$ grow exponentially as the PCA dynamics becomes less noisy. Right panel: behavior of $\tau(L, \alpha)$ with the system size L . Points correspond to averages over 1000 samples. While $\tau(L, \alpha)$ clearly diverges as $\alpha \searrow 0$, it does not so as L grows at least down to $\alpha = 0.025$.

cells in the state \leftarrow ($N_{\leftarrow}(\tau) > L/2$) is observed, signaling that the PCA “crossed” the “potential barrier.” We then obtain the flipping time $\tau(L, \alpha)$ for each given L and α as an average of 1000 such hitting times. In our simulations $80 \leq L \leq 400$ and $0.024 \leq \alpha \leq 0.100$. The relatively small L allow us to investigate the flipping times without having to wait too much to observe the flips. Our results appear in Figure 5.

The behavior of $\tau(L, \alpha)$ with α seems to indicate that the PCA is nonergodic at least up to $\alpha \lesssim 0.05$. Otherwise, we do not observe any sign of divergence of $\tau(L, \alpha)$ with increasing L up to $L = 400$ and down to $\alpha = 0.025$, indicating that the PCA is likely to be ergodic in these regions of parameters. The best that we can do with these mixed signals, then, is to combine the bound $\alpha \leq 0.025$ provided by the behavior of $\tau(L, \alpha)$ with L together with the bound $\alpha_c \lesssim 0.018$ provided by Figure 3 to set an upper bound on the critical level of noise separating the ergodic from the nonergodic phase of GKL-IV, if any, at $\alpha_c \approx 0.018$.

5 Summary and conclusions

We found that the GKL-IV model performs well in the density classification problem, with a performance comparable with that of the more well-known model GKL-II. In fact, GKL-IV performs slightly better at the task, even having more states to deal with. The additional states \uparrow and \downarrow enable GKL-IV to annihilate isolated \leftarrow and \rightarrow states and create local islands of majority states \uparrow and \downarrow that are then eroded from the boundaries by means of transitions involving the states \leftarrow and \rightarrow that propagate twice as fast as the former processes, thus leading the CA to converge to the majority state among these states. This somewhat elaborate eroder mechanism turns out to be very effective. On the negative side, GKL-IV takes longer (almost 3 times more,

see Figure 1) to reach consensus. If performance is to be preferred over speed, however, than GKL-IV is a better classifier than GKL-II at only a moderate increase in time.

We also investigated the performance of GKL-IV under the influence of noise and found signs of an ergodic-nonergodic phase transition at some small finite positive level of noise. Indeed, from Figure 3 we see that the stationary density of \rightarrow states clearly becomes bimodal below $\alpha \approx 0.05$, indicating that GKL-IV apparently becomes nonergodic for levels of noise below this value, but the exact location of α_c is not very clear from that figure. The behavior of the flipping times $\tau(L, \alpha)$ displayed in Figure 5 also indicate that GKL-IV is probably nonergodic for $\alpha < 0.05$, although the behavior of this quantity with the system size L indicate that the system is ergodic at least down to $\alpha \approx 0.025$. Combining this somewhat conflicting informations together with the fact that flipping between the two majority phases ceases completely about $\alpha \approx 0.018$, the best that we can do is to set $\alpha_c \lesssim 0.018$ as an upper bound on the critical point for a putative ergodic-nonergodic phase transition of GKL-IV. Note that estimates of α_c from Figures 3 and 5 are affected by the finite size of the system and the finite time of the simulations. Our data indicate that GKL-IV may be ergodic but are not conclusive; large systems simulated for longer periods could tell better.

In [2] the authors advanced the idea that GKL-IV (as well as its siblings GKL-II and GKL-VI) under noise is “quasinonergodic,” in the sense that while the models are ergodic for any $\alpha > 0$, convergence to the unique invariant measure is extremely slow. The behavior displayed by $\langle N_{\rightarrow} \rangle / L$ and $\tau(L, \alpha)$ in Figures 3 and 5 seem to support this idea. Otherwise, recent results indicate that the ergodicity of one-dimensional PCA is in general undecidable [12, 42, 43]. We were able to set an upper bound on the critical level of noise of GKL-IV above which it becomes ergodic. Whether this critical level is even smaller or zero remains an open question.

The GKL-II and IV CA and PCA deserve a more extensive analytical study. We believe that already at the level of pair (two-cell) mean field approximations [47, 48] the equations may reveal an interesting structure. In the same vein, a study of the spreading of damage [49, 50] in the GKL-II and IV PCA may help to clarify the rate of convergence of the dynamics to the steady states and help to understand CA and PCA that are able to classify density.

Acknowledgments

The authors are pleased to thank Peter Gacs (BU) for useful correspondence, library specialist Angela K. Gruendl (UIUC) for excellent service in providing a copy of reference [3], and Yeva Gevorgyan (USP) for help with the literature in Russian. This work was partially supported by FAPESP, the São Paulo State Research Foundation, under grant 2015/21580-0 and by CNPq, the Brazilian National Council of Scientific and Technological Development, through Ph. D. grant 140684/2016-6.

A Complete GKL-IV rule table

We had to tinker a bit with GKL-IV before getting its rule table from [2] right, so we share the result of our work here. Table I displays all the elementary transitions of GKL-IV according to rules (1a)–(1c) supplemented by their reflections (2) as described in Section 2.

References

- [1] G. L. Kurdyumov, An example of a nonergodic homogeneous one-dimensional random medium with positive transition probabilities, *Sov. Math. Dokl.* **19**(1), 211–214 (1978).
- [2] P. Gach, G. L. Kurdyumov, L. A. Levin, One-dimensional uniform arrays that wash out finite islands, *Probl. Inform. Transm.* **14**(3), 223–226 (1978).
- [3] N. B. Vasil’ev, R. L. Dobrushin, I. I. Pyatetskii-Shapiro, Markov processes on an infinite product of discrete spaces, in: *Soviet-Japanese Symposium on Probability Theory*, Khabarovsk, USSR, August 1969, Proceedings (Akad. Nauk SSSR, Novosibirsk, 1969), Part 1, Vol. 2: Soviet Contributions, pp. 3–30 (in Russian).
- [4] N. B. Vasil’ev, M. B. Petrovskaya, I. I. Pyatetskii-Shapiro, Modelling of voting with random error, *Automat. Rem. Contr.* **30**(10), 1639–1642 (1970).
- [5] L. N. Vaserstein, Markov processes over denumerable products of spaces, describing large systems of automata, *Probl. Inform. Transm.* **5**(3), 47–52 (1969).
- [6] A. V. Kuznetsov, Information storage in a memory assembled from unreliable components, *Probl. Inform. Transm.* **9**(3), 254–264 (1973).
- [7] O. N. Stavskaya, Gibbs invariant measures for Markov chains on finite lattices with local interaction, *Math. USSR Sb.* **21**(3), 395–411 (1973).
- [8] A. L. Toom, Nonergodic multidimensional system of automata, *Probl. Inform. Transm.* **10**(3), 239–246 (1974).
- [9] O. N. Stavskaya, Sufficient conditions for the uniqueness of a probability field and estimates for correlations, *Math. Not. Acad. Sci. USSR* **18**(4), 950–956 (1975).
- [10] B. S. Cirel’son, Reliable storage of information in a system of unreliable components with local interactions, in: R. L. Dobrushin, V. I. Kryukov, A. L. Toom (Eds.), *Locally Interacting Systems and their Application in Biology*, Proceedings of the School-Seminar on Markov Interaction Processes in Biology, Pushchino, Moscow Region, USSR, March 1976 (Springer, New York/Berlin, 1978), pp. 15–30.

Table I: Elementary transitions of GKL-IV. When a transition is defined by more than one rule, only the first rule that defines it is listed. Transitions obtained by reflection of some rule have the respective rule marked by an asterisk.

(x_{i-1}, x_i, x_{i+1})	x'_i	Rule	(x_{i-1}, x_i, x_{i+1})	x'_i	Rule
$(\rightarrow, \rightarrow, \rightarrow)$	\rightarrow	(1a)	$(\rightarrow, \leftarrow, \rightarrow)$	\downarrow	(1b)*
$(\rightarrow, \rightarrow, \leftarrow)$	\rightarrow	(1b)	$(\rightarrow, \leftarrow, \leftarrow)$	\leftarrow	(1b)*
$(\rightarrow, \rightarrow, \uparrow)$	\rightarrow	(1a)	$(\rightarrow, \leftarrow, \uparrow)$	\downarrow	(1b)*
$(\rightarrow, \rightarrow, \downarrow)$	\rightarrow	(1a)	$(\rightarrow, \leftarrow, \downarrow)$	\leftarrow	(1b)*
$(\leftarrow, \rightarrow, \rightarrow)$	\downarrow	(1b)	$(\leftarrow, \leftarrow, \rightarrow)$	\downarrow	(1b)*
$(\leftarrow, \rightarrow, \leftarrow)$	\downarrow	(1b)	$(\leftarrow, \leftarrow, \leftarrow)$	\leftarrow	(1a)*
$(\leftarrow, \rightarrow, \uparrow)$	\downarrow	(1b)	$(\leftarrow, \leftarrow, \uparrow)$	\downarrow	(1b)*
$(\leftarrow, \rightarrow, \downarrow)$	\downarrow	(1b)	$(\leftarrow, \leftarrow, \downarrow)$	\leftarrow	(1b)*
$(\uparrow, \rightarrow, \rightarrow)$	\downarrow	(1b)	$(\uparrow, \leftarrow, \rightarrow)$	\downarrow	(1b)*
$(\uparrow, \rightarrow, \leftarrow)$	\downarrow	(1b)	$(\uparrow, \leftarrow, \leftarrow)$	\leftarrow	(1a)*
$(\uparrow, \rightarrow, \uparrow)$	\downarrow	(1b)	$(\uparrow, \leftarrow, \uparrow)$	\downarrow	(1b)*
$(\uparrow, \rightarrow, \downarrow)$	\downarrow	(1b)	$(\uparrow, \leftarrow, \downarrow)$	\leftarrow	(1b)*
$(\downarrow, \rightarrow, \rightarrow)$	\rightarrow	(1b)	$(\downarrow, \leftarrow, \rightarrow)$	\downarrow	(1b)*
$(\downarrow, \rightarrow, \leftarrow)$	\rightarrow	(1b)	$(\downarrow, \leftarrow, \leftarrow)$	\leftarrow	(1a)*
$(\downarrow, \rightarrow, \uparrow)$	\rightarrow	(1b)	$(\downarrow, \leftarrow, \uparrow)$	\downarrow	(1b)*
$(\downarrow, \rightarrow, \downarrow)$	\rightarrow	(1b)	$(\downarrow, \leftarrow, \downarrow)$	\leftarrow	(1b)*
$(\rightarrow, \uparrow, \rightarrow)$	\rightarrow	(1a)	$(\rightarrow, \downarrow, \rightarrow)$	\rightarrow	(1a)
$(\rightarrow, \uparrow, \leftarrow)$	\uparrow	(1c)	$(\rightarrow, \downarrow, \leftarrow)$	\uparrow	(1c)
$(\rightarrow, \uparrow, \uparrow)$	\rightarrow	(1a)	$(\rightarrow, \downarrow, \uparrow)$	\rightarrow	(1a)
$(\rightarrow, \uparrow, \downarrow)$	\rightarrow	(1a)	$(\rightarrow, \downarrow, \downarrow)$	\rightarrow	(1a)
$(\leftarrow, \uparrow, \rightarrow)$	\uparrow	(1c)	$(\leftarrow, \downarrow, \rightarrow)$	\uparrow	(1c)
$(\leftarrow, \uparrow, \leftarrow)$	\leftarrow	(1a)*	$(\leftarrow, \downarrow, \leftarrow)$	\leftarrow	(1a)*
$(\leftarrow, \uparrow, \uparrow)$	\uparrow	(1c)	$(\leftarrow, \downarrow, \uparrow)$	\uparrow	(1c)
$(\leftarrow, \uparrow, \downarrow)$	\uparrow	(1c)	$(\leftarrow, \downarrow, \downarrow)$	\uparrow	(1c)
$(\uparrow, \uparrow, \rightarrow)$	\uparrow	(1c)	$(\uparrow, \downarrow, \rightarrow)$	\uparrow	(1c)
$(\uparrow, \uparrow, \leftarrow)$	\leftarrow	(1a)*	$(\uparrow, \downarrow, \leftarrow)$	\leftarrow	(1a)*
$(\uparrow, \uparrow, \uparrow)$	\uparrow	(1c)	$(\uparrow, \downarrow, \uparrow)$	\uparrow	(1c)
$(\uparrow, \uparrow, \downarrow)$	\uparrow	(1c)	$(\uparrow, \downarrow, \downarrow)$	\uparrow	(1c)
$(\downarrow, \uparrow, \rightarrow)$	\uparrow	(1c)	$(\downarrow, \downarrow, \rightarrow)$	\uparrow	(1c)
$(\downarrow, \uparrow, \leftarrow)$	\leftarrow	(1a)*	$(\downarrow, \downarrow, \leftarrow)$	\leftarrow	(1a)*
$(\downarrow, \uparrow, \uparrow)$	\uparrow	(1c)	$(\downarrow, \downarrow, \uparrow)$	\uparrow	(1c)
$(\downarrow, \uparrow, \downarrow)$	\uparrow	(1c)	$(\downarrow, \downarrow, \downarrow)$	\uparrow	(1c)

- [11] A. L. Toom, Stable and attractive trajectories in multicomponent systems, in: R. L. Dobrushin, Ya. G. Sinai (Eds.), *Advances in Probability Vol. 6* (Marcel Dekker, New York, 1980), pp. 549–576.
- [12] A. L. Toom, N. B. Vasilyev, O. N. Stavskaya, L. G. Mityushin, G. L. Kurdyumov, S. A. Pirogov, Discrete local Markov systems, in: R. L. Dobrushin, V. I. Kryukov, A. L. Toom (Eds.), *Stochastic Cellular Systems: Ergodicity, Memory, Morphogenesis* (Manchester University Press, Manchester, 1990), pp. 1–182.
- [13] R. Holley, D. W. Stroock, In one and two dimensions, every stationary measure for a stochastic Ising model is a Gibbs state, *Commun. Math. Phys.* **55** (1), 37–45 (1977).
- [14] C. H. Bennett, G. Grinstein, Role of irreversibility in stabilizing complex and nonergodic behavior in locally interacting discrete systems, *Phys. Rev. Lett.* **55** (7), 657–660 (1985).
- [15] C. H. Bennett, Dissipation, anisotropy, and the stabilization of computationally complex states of homogeneous media, *Physica A* **163** (1), 393–397 (1990).
- [16] G. Grinstein, Can complex structures be generically stable in a noisy world?, *IBM J. Res. & Dev.* **48** (1), 5–12 (2004).
- [17] J. A. Cuesta, A. Sánchez, General non-existence theorem for phase transitions in one-dimensional systems with short range interactions, and physical examples of such transitions, *J. Stat. Phys.* **115** (3–4), 869–893 (2004).
- [18] A. Georges, P. Le Doussal, From equilibrium spin models to probabilistic cellular automata, *J. Stat. Phys.* **54** (3), 1011–1064 (1989).
- [19] J. L. Lebowitz, C. Maes, E. R. Speer, Statistical mechanics of probabilistic cellular automata, *J. Stat. Phys.* **59** (1), 117–190 (1990).
- [20] P. Gonzaga de Sá, C. Maes, The Gacs-Kurdyumov-Levin automaton revisited, *J. Stat. Phys.* **67** (3–4), 507–522 (1992).
- [21] P. Gács, Reliable computation with cellular automata, *J. Comput. Syst. Sci.* **32** (1), 15–78 (1986).
- [22] P. Gács, Reliable cellular automata with self-organization, *J. Stat. Phys.* **103** (1–2), 45–267 (2001).
- [23] L. F. Gray, A reader’s guide to Gács’s ‘positive rates’ paper, *J. Stat. Phys.* **103** (1–2), 1–44 (2001).

- [24] M. R. Evans, D. P. Foster, C. Godreche, D. Mukamel, Spontaneous symmetry breaking in a one dimensional driven diffusive system, *Phys. Rev. Lett.* **74** (2), 208–211 (1995).
- [25] M. R. Evans, Y. Kafri, H. M. Koduvely, D. Mukamel, Phase separation in one-dimensional driven diffusive systems, *Phys. Rev. Lett.* **80** (3), 425–429 (1998).
- [26] M. R. Evans, Phase transitions in one-dimensional nonequilibrium systems, *Braz. J. Phys.* **30** (1), 42–57 (2000).
- [27] A. Rákos, M. Paessens, Ergodicity breaking in one-dimensional reaction-diffusion systems, *J. Phys. A: Math. Gen.* **39** (13), 3231–3252 (2006).
- [28] A. Rákos, M. Paessens, G. M. Schütz, Broken ergodicity in driven one-dimensional particle systems with short-range interaction, *Markov Proc. Rel. Fields* **12**, 309–322 (2006).
- [29] M. Mitchell, P. T. Hraber, J. P. Crutchfield, Revisiting the edge of chaos: Evolving cellular automata to perform computations, *Complex Systems* **7** (2), 89–130 (1993).
- [30] J. P. Crutchfield, M. Mitchell, The evolution of emergent computation, *Proc. Natl. Acad. Sci. USA* **92** (23), 10742–10746 (1995).
- [31] H. Fukás, Solution of the density classification problem with two cellular automata rules, *Phys. Rev. E* **55** (3), R2081–R2084 (1997).
- [32] M. Sipper, M. S. Capcarrere, E. Ronald, A simple cellular automaton that solves the density and ordering problems, *Int. J. Mod. Phys. C* **9** (7), 899–902 (1998).
- [33] B. Mesota, C. Teuscherb, Deducing local rules for solving global tasks with random Boolean networks, *Physica D* **211** (1–2), 88–106 (2005).
- [34] A. A. Moreira, A. Mathur, D. Diermeier, L. A. N. Amaral, Efficient system-wide coordination in noisy environments, *Proc. Natl. Acad. Sci. USA* **101** (33), 12085–12090 (2004).
- [35] S. M. D. Seaver, A. A. Moreira, M. Sales-Pardo, R. D. Malmgren, D. Diermeier, L. A. N. Amaral, Micro-bias and macro-performance, *Eur. Phys. J. B* **67** (3), 369–375 (2009).
- [36] R. Briceño, P. M. de Espanés, A. Osses, I. Rapaport, Solving the density classification problem with a large diffusion and small amplification cellular automaton, *Physica D* **261**, 70–80 (2013).
- [37] C. Stone, L. Bull, Evolution of cellular automata with memory: The density classification task, *BioSystems* **97** (2), 108–116 (2009).

- [38] J. R. G. Mendonça, Monte Carlo investigation of the critical behavior of Stavskaya's probabilistic cellular automaton, *Phys. Rev. E* **83** (1), 012102 (2011).
- [39] J. R. G. Mendonça, Sensitivity to noise and ergodicity of an assembly line of cellular automata that classifies density, *Phys. Rev. E* **83** (3), 031112 (2011).
- [40] N. Fatès, Stochastic cellular automata solutions to the density classification problem – When randomness helps computing, *Theory Comput. Syst.* **53** (2), 223–242 (2013).
- [41] J. Mairesse, I. Marcovici, Around probabilistic cellular automata, *Theor. Comput. Sci.* **559**, 42–72 (2014).
- [42] A. Bušić, J. Mairesse, I. Marcovici, Probabilistic cellular automata, invariant measures, and perfect sampling, *Adv. Appl. Probab.* **45** (4), 960–980 (2013).
- [43] I. Marcovici, Ergodicity of noisy cellular automata: The coupling method and beyond, in: A. Beckmann, L. Bienvenu, N. Jonoska (Eds.), *Pursuit of the Universal: 12th Conference on Computability in Europe, CiE 2016*, Paris, France, June 27–July 1, 2016, Proceedings (Springer, Cham, 2016), pp. 153–163.
- [44] P. P. B. de Oliveira, J. C. Bortot, G. M. B. Oliveira, The best currently known class of dynamically equivalent cellular automata rules for density classification, *Neurocomputing* **70** (1–3), 35–43 (2006).
- [45] P. P. B. de Oliveira, On density determination with cellular automata: Results, constructions and directions, *J. Cell. Autom.* **9** (5–6), 357–385 (2014).
- [46] J. R. G. Mendonça, Mean-field critical behavior and ergodicity break in a nonequilibrium one-dimensional RSOS growth model, *Int. J. Mod. Phys. C* **23** (3), 1250019 (2012).
- [47] J. Marro, R. Dickman, *Nonequilibrium Phase Transitions in Lattice Models* (Cambridge University Press, Cambridge, 1999).
- [48] P. Balister, B. Bollobás, R. Kozma, Large deviations for mean field models of probabilistic cellular automata, *Random Struct. Algor.* **29** (3), 399–415 (2006).
- [49] G. A. Kohring, M. Schreckenberg, The Domany-Kinzel cellular automaton revisited, *J. Phys. I (France)* **2** (11), 2033–2037 (1992).
- [50] T. Tomé, Spreading of damage in the Domany-Kinzel cellular automaton: A mean-field approach, *Physica A* **212** (1–2), 99–109 (1994).